

Electronic Supplementary Information

Enhanced Cycle Life and Capacity Retention of Iron Oxide Ultrathin Film Coated SnO₂ Nanoparticles at High Current Densities

Sai Abhishek Palaparty[†], Rajankumar L. Patel[†], Xinhua Liang^{*}

Department of Chemical and Biochemical Engineering, Missouri University of Science and Technology, Rolla, MO 65409, USA

[†] These authors contributed equally.

^{*} Corresponding author, Email: liangxin@mst.edu

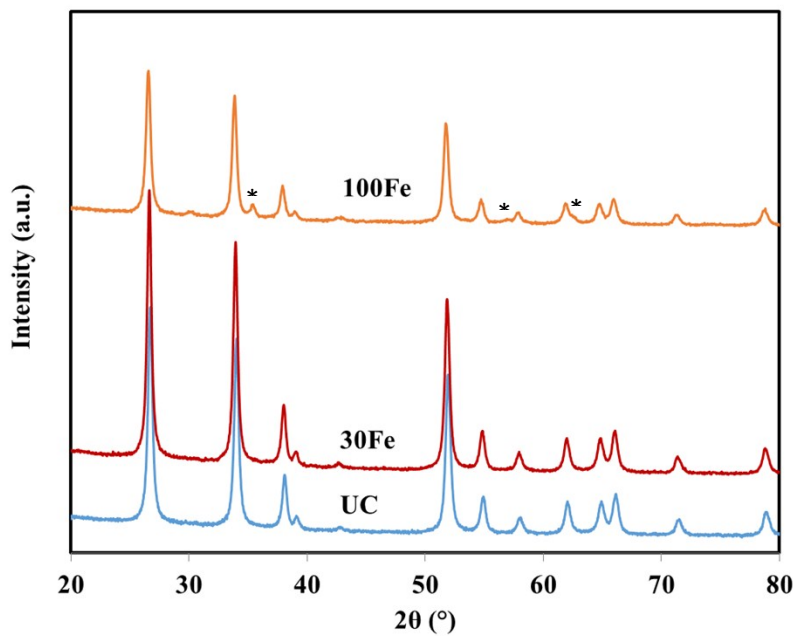


Figure S1. XRD spectra of the uncoated (UC), 30 cycles of iron oxide ALD (30Fe), and 100 cycles of iron oxide ALD (100Fe) coated SnO₂ particles. * represents new peaks with low intensity.

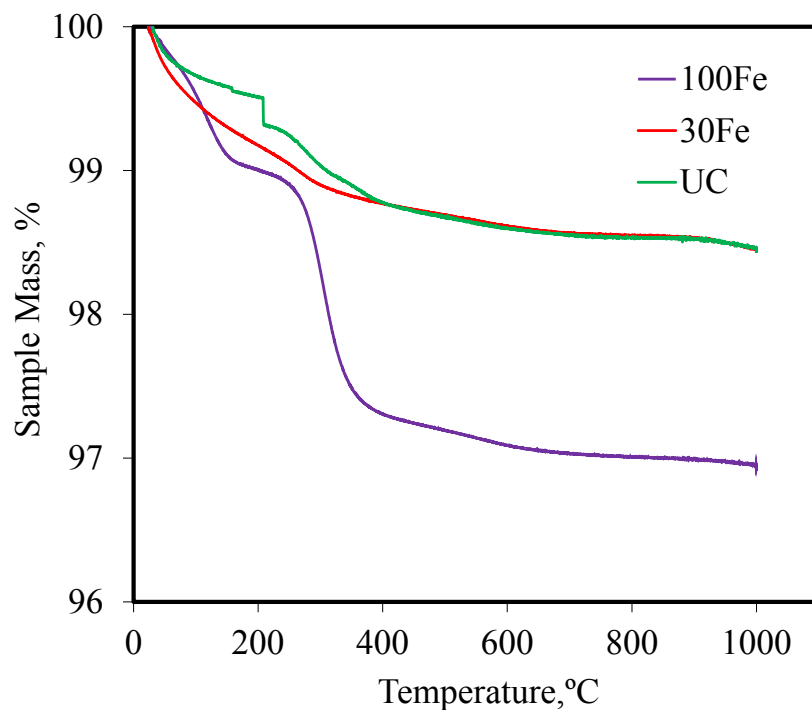


Figure S2. Thermogravimetric analysis (TGA) of the uncoated (UC), 30 cycles of iron oxide ALD (30Fe), and 100 cycles of iron oxide ALD (100Fe) coated SnO_2 particles performed under O_2 with a step increase of $10^\circ\text{C}/\text{min}$.

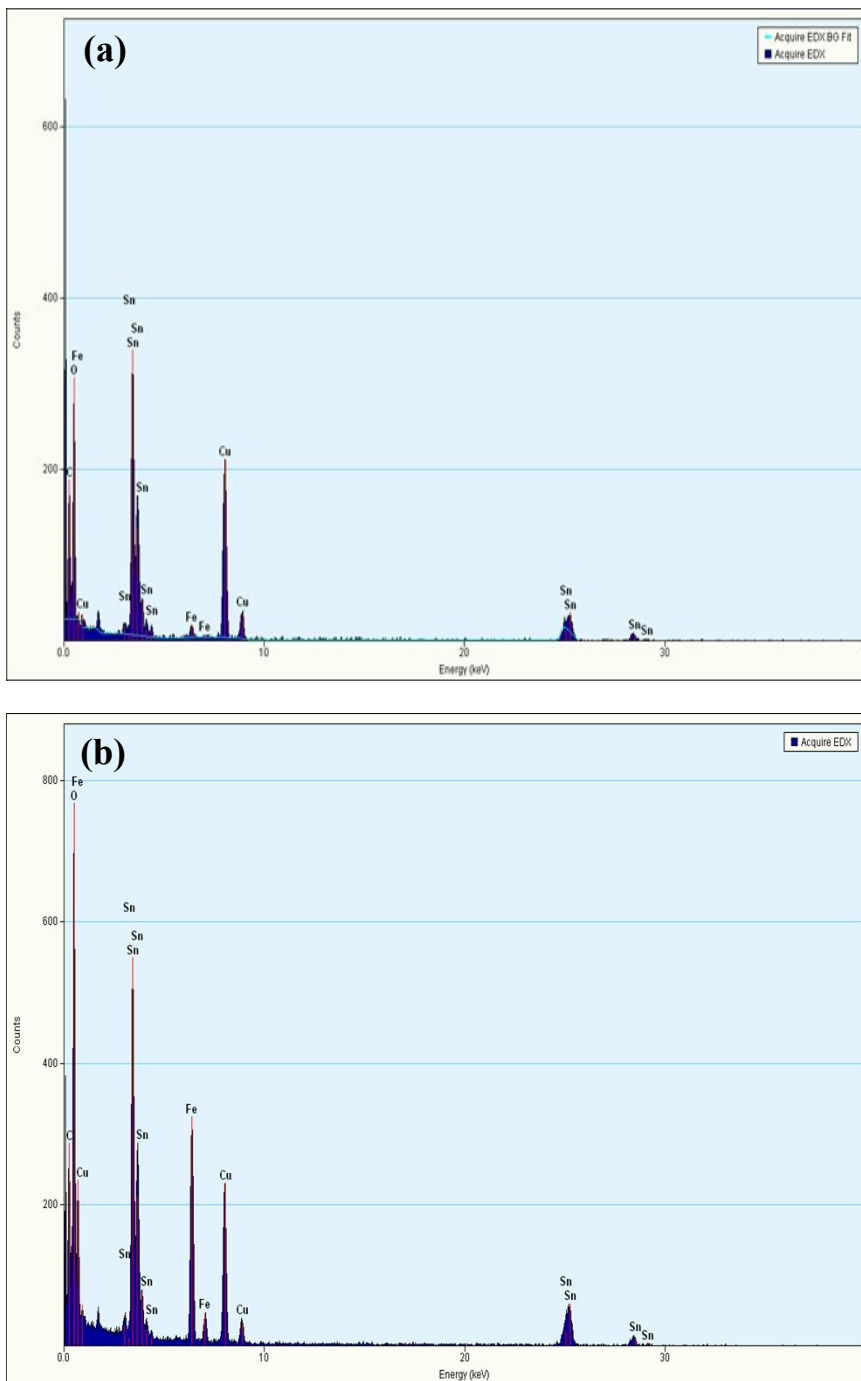


Figure S3. EDS spectra of (a) 30Fe, and (b) 100Fe coated SnO_2 particles.

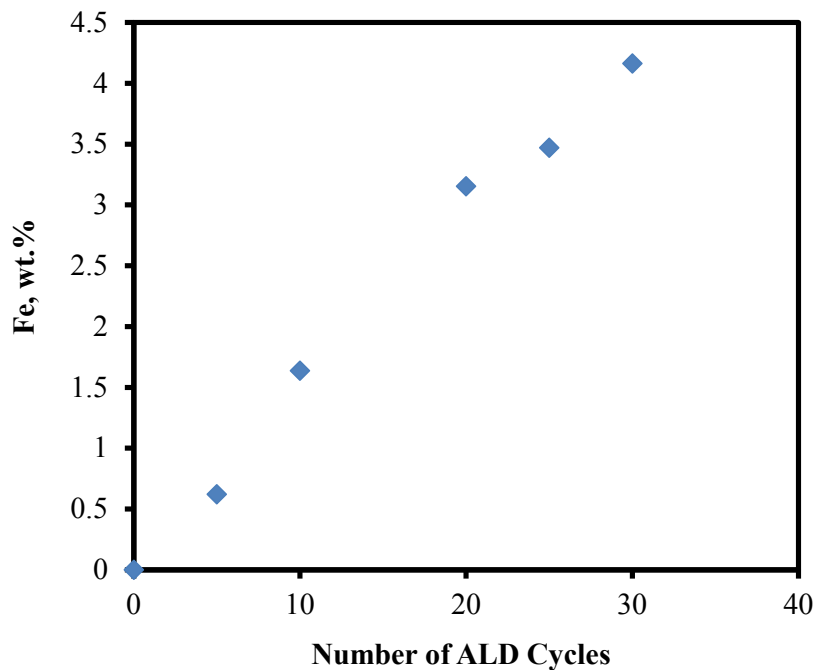


Figure S4. Fe content versus the number of iron oxide ALD coating cycles, as obtained from ICP-AES analysis.

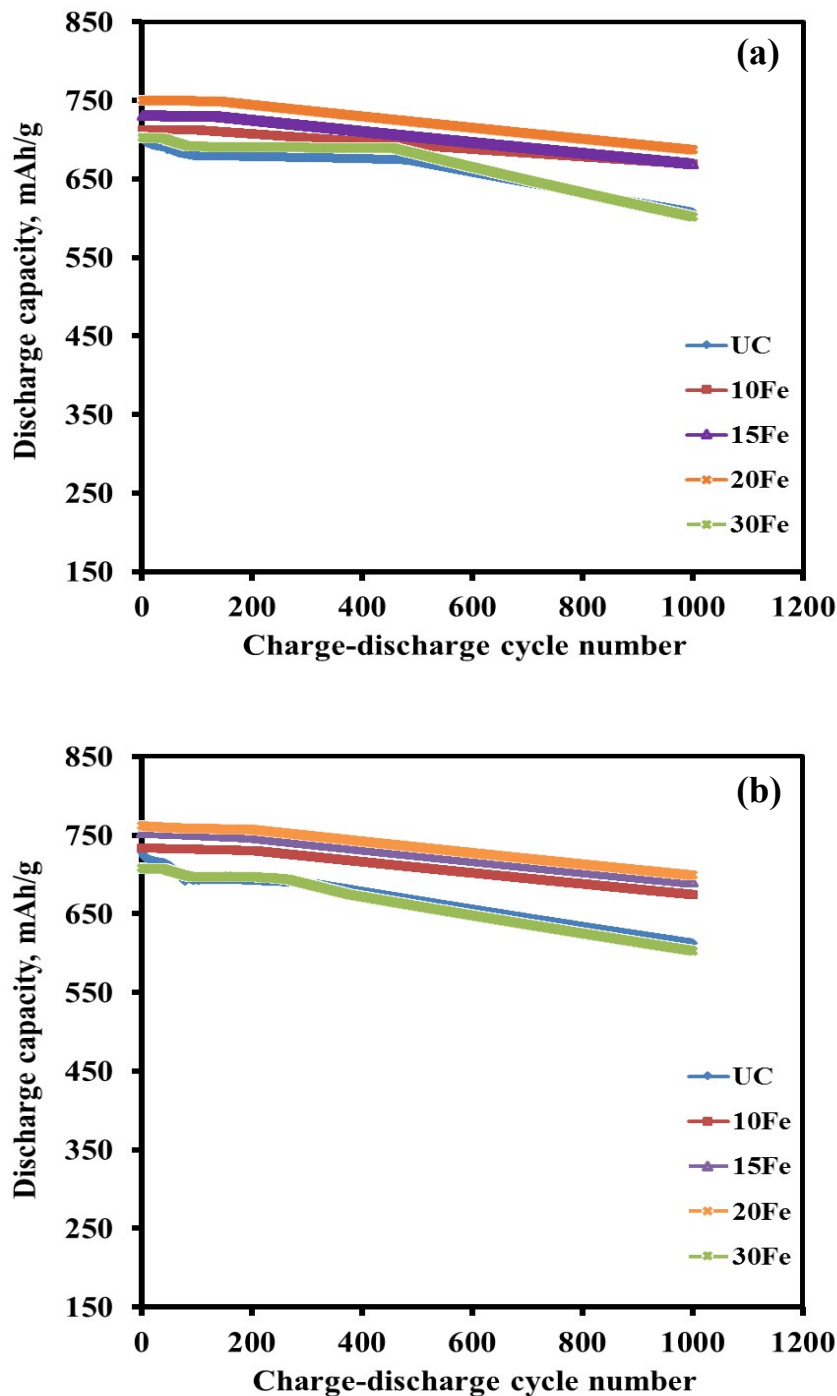


Figure S5. Galvanostatic discharge capacities of SnO_2 particles coated with various thicknesses of iron oxide ALD films at a current density of 250 mA/g between 0.5-3 V at (a) room temperature and (b) 55 °C.

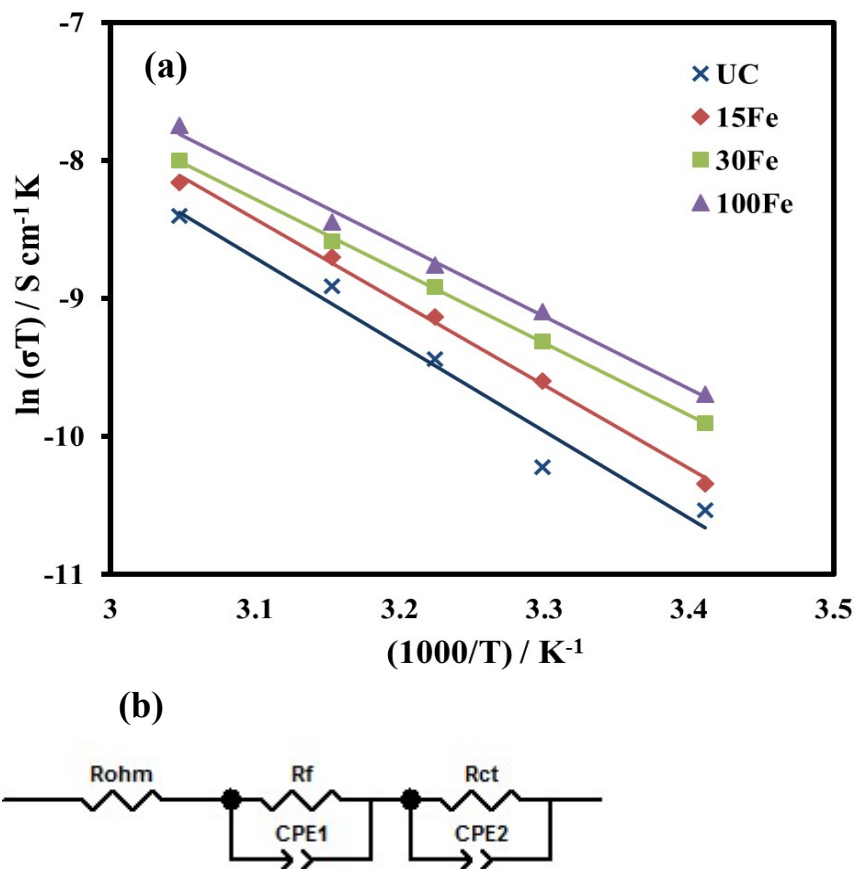


Figure S6. (a) Arrhenius plot of uncoated and 15Fe, 30Fe, 100Fe coated SnO_2 particles for the effects of temperature on conductivity, (b) equivalent circuit for impedance spectra.

Iron oxide film phase characterization

XRD analysis was performed on the 30Fe and 100Fe samples to determine the phase of iron oxide ALD films deposited on tin oxide particles. The XRD spectra of the 30Fe and 100Fe samples were compared to that of the uncoated (UC) sample (Figure S1). In both spectra, the diffraction peaks at 26.5, 33.8, 38.2, 51.8, 54.8, 58.2, 61.7, 64.8, 66.1, 71.8 and 78.8° depict the (110), (101), (200), (211), (220), (002), (310), (112), (301), (202) and (321) crystal planes of the rutile phase SnO_2 (JCPDS No. 41-1445). The XRD analysis showed that there was no significant difference between the spectra of the UC and 30Fe samples. The observation of similarity in XRD spectra of iron oxide coated and uncoated SnO_2 particles was also reported by El-Shiwani et al.¹ However, the XRD analysis of the 100Fe sample showed evidence of low intensity new peaks (denoted by * in Figure S1) at 30.9 and 61.8°, corresponding to (220) and (440) crystal planes of Fe_3O_4 (JCPDS No. 75-0033). These peaks also match with (220) and (440) planes of $\alpha\text{-Fe}_2\text{O}_3$ (JCPDS No. 80-2377). Hence, in this study, the phase of the iron oxide in the ultrathin film cannot be interpreted without ambiguity. The other low intensity new peak at 37.9° can match with any form or phase of iron oxide. Khalr and coworkers² also observed that XRD spectra of thin iron oxide coating on fluorine doped tin oxide (FTO) by ALD had weak signals for iron oxide and hence, the phase could not be interpreted without ambiguity.

Thermogravimetric analysis (TGA) under O_2 with a step increase of 10°C/min was performed on the 30Fe and 100Fe sample to interpret the phase of iron oxide (Figure S2). The TGA curve of the UC sample was used as a baseline to compare the 30Fe and the 100Fe samples. For all the samples, the initial weight loss occurred due to removal of physically adsorbed water. The TGA curves of the 30Fe and the UC samples show a total weight loss of ~1.6% at 400°C, which is mainly due to

loss of physically adsorbed water (< 200°C) and dehydration of surface hydroxyl groups (> 200°C). Above 400°C, the curve remains stable with no apparent weight loss or gain. In case of the 100Fe sample, the total weight loss was higher at ~3%, most of which had already occurred at 400°C. Above this temperature, the curves show no apparent weight loss or gain. If there was mass gain, the phase of iron oxide would be FeO or Fe₃O₄ as there would be mass gain from its oxidation. The oxidation of FeO to Fe₃O₄ or Fe₃O₄ to Fe₂O₃ normally occurs above 120°C and 200°C in presence of oxygen respectively. However, there was no mass gain observed in the TGA curves of both the 30Fe and the 100 Fe samples. Theoretically, by using the content of Fe from the ICP-AES data and assuming the film to be entirely Fe₃O₄, the expected mass gain in case of the 30Fe and the 100 Fe samples is 0.19 % and 0.38 % respectively. Assuming the film to be entirely FeO, the mass gain in case of the 30Fe and the 100 Fe samples is 0.59 % and 1.14 %, respectively. This expected mass gain is less than the mass loss of water removal and hence cannot be seen in the TGA curves. The higher mass loss in case of the 100Fe sample was due to presence of more surface hydroxyl groups because of thicker iron oxide film. Herein, since the phase of iron oxide could not be confidently identified, which is similar to the XRD results and hence, it is referred as FeO_x in the paper.

Conductivity measurements

Pellets of only UC, 15Fe, 30Fe and 100Fe samples were prepared for mixed ionic and electronic conductivity measurements. The ac complex plane impedance experiment as described in our previous work was conducted on these samples.³ The impedance planes were obtained using the same impedance analyzer that was used to measure the EIS spectra. Figure S6b depicts the equivalent circuit that was used to fit the impedance spectra. Out of all the samples, the 100Fe

sample showed the highest mixed conductivity (Figure S6a). The conductivity plot is found to be linear and to obey the Arrhenius equation,

$$\sigma \cdot T = \sigma_0 \cdot \exp\left(\frac{-E_a}{k_B T}\right)$$

where, σ_0 is the pre-exponential factor, k_B is the Boltzmann constant, T is the absolute temperature, and E_a is the activation energy for Li ion movement. Figure S6a shows the direct correlation between the mixed conductivity and the temperature (a linear Arrhenius plot). Since the testing temperature were limited to 328 K, there was no phase or structural change observed during the measurements.

References

1. H. El-Shinawi, A. S. Schulze, M. Neumeier, T. Leichtweiß and J. Janek, *The Journal of Physical Chemistry C*, 2014, **118**, 8818-8823.
2. B. M. Klahr, A. B. F. Martinson and T. W. Hamann, *Langmuir*, 2011, **27**, 461-468.
3. R. L. Patel, H. Xie, J. Park, H. Y. Asl, A. Choudhury and X. Liang, *Advanced Materials Interfaces*, 2015, **2**, 1500046